

## Accepted Manuscript

On the reliability of serviceability calculations for flexural cracked reinforced concrete beams

Tengfei Xu, Arnaud Castel, R. Ian Gilbert

PII: S2352-0124(18)30001-8  
DOI: doi:[10.1016/j.istruc.2018.01.001](https://doi.org/10.1016/j.istruc.2018.01.001)  
Reference: ISTRUC 245

To appear in:

Received date: 31 July 2017  
Revised date: 29 December 2017  
Accepted date: 7 January 2018

Please cite this article as: Xu Tengfei, Castel Arnaud, Gilbert R. Ian, On the reliability of serviceability calculations for flexural cracked reinforced concrete beams, (2018), doi:[10.1016/j.istruc.2018.01.001](https://doi.org/10.1016/j.istruc.2018.01.001)

This is a PDF file of an unedited manuscript that has been accepted for publication. As a service to our customers we are providing this early version of the manuscript. The manuscript will undergo copyediting, typesetting, and review of the resulting proof before it is published in its final form. Please note that during the production process errors may be discovered which could affect the content, and all legal disclaimers that apply to the journal pertain.



# On the reliability of serviceability calculations for flexural cracked reinforced concrete beams

Tengfei Xu<sup>a,b,\*</sup>, Arnaud Castel<sup>c</sup>, R. Ian Gilbert<sup>c</sup>

<sup>a</sup>*Department of Bridge Engineering, Southwest Jiaotong University, Chengdu 610031, P.R. China*

<sup>b</sup>*Key Laboratory of High-speed Railway Engineering, Ministry of Education,  
Southwest Jiaotong University, Chengdu 610031, P.R. China*

<sup>c</sup>*Centre for Infrastructure Engineering and Safety, School of Civil and Environmental Engineering,  
The University of New South Wales, UNSW Sydney, NSW 2052, Australia*

---

## Abstract

Under in-service conditions, beams and slabs in reinforced concrete structures are almost always cracked, as the tensile strength of the concrete is low. Due to the irreversible reduction in overall stiffness resulting from cracking and the residual deflection after unloading, the structural response is load path dependent. In this paper, an existing average moment of inertia model and Monte Carlo simulation (MCS) are adopted to take into account the effect of historical cracking damage on the reliability of serviceability calculations for reinforced concrete (RC) members. The suitability of the average moment of inertia model for reliability analysis is verified by considering experimental tests on a total of eleven reinforced concrete beams. The errors associated with both the effective and average moment of inertia predicted by the model are calibrated using the experimental data. By using the proposed approach to account for the various sources of uncertainty in reinforced concrete beams, the quantitative loss in the short-term and long-term serviceability reliability of a cracked reinforced concrete beam was calculated. The results confirm

---

\*Corresponding author. soar1120@gmail.com

that the effect of historical cracking damage on short-term serviceability reliability should be taken into account when the deflection induced by historical loading is larger than the deflection limitation. Light historical damage has no influence on the short-term serviceability reliability, although it affects the probability density distribution of the deflection. However, in the long-term serviceability reliability analysis, even when the historical damage is light, the long-term serviceability reliability index is decreased as the cracking damage to the stiffness affects the time-dependent deflection. Additionally, the later a damaging load is applied to a reinforced concrete beam, the less is the influence of cracking damage on the long-term serviceability reliability.

*Keywords:* Reinforced concrete, tension stiffening, serviceability, reliability, moment of inertia

---

## 1. Introduction

Due to the random nature of the quantities affecting the structural behaviour (e.g. actions, geometry, restraints, and strength of materials), the assessment of structural performance requires a probabilistic rather than a deterministic approach and an assessment of the reliability of design calculations, particularly under in-service conditions[1]. Indeed, probability-based limit-state design is accepted in codes for reinforced concrete design throughout the world.

Structural safety and serviceability are two broad classifications of the performance requirements for structures. Structural safety is the ability to estimate the overall stability, ductility and ultimate bearing resistance corresponding to a set of assumed design actions with appropriate levels of reliability. Using probabilistic methods in conjunction with the finite element method (FEM), many reliability analyses have been proposed to deal with the ultimate limit state of RC structures [2–9]. Compared to structural safety, the serviceability problem, relating to deflection, crack width, vibration, and degree of spalling [1], are much more difficult to define. Considerations of serviceability are based on subjective issues, such as human perception and tolerances, the importance of the structure and the consequences of serviceability problems and are more client-oriented [10]. Moreover, in modern times, the introduction of high-strength materials has led to more slender structural elements and has made serviceability issues of increasing importance. Under in-service conditions, reinforced concrete structural members are almost always cracked, as the tensile strength of the concrete is low. Cracking affects the stiffness of a RC member and hence its deflection. Therefore, it is important to assess RC-members after cracking in any serviceability analysis.

Under normal service conditions, the concrete between the primary cracks in a

beam is able to continue to carry tensile stress, due to the transfer of forces from the tensile reinforcement to the concrete through bond. This phenomenon is known as tension stiffening and must be accurately modeled to simulate the in-service behavior of reinforced concrete structures, particularly under repeated loading [11].

Most of existing models for assessing the loss of stiffness due to cracking in reinforced concrete beams are concerned with monotonic loading. The smeared-crack model is a popular way to simulate the tension stiffening effect. In this approach, an average stress-strain relation is considered for the whole tension area to account for the average deformation response after cracking [12]. A modified constitutive relationship for the steel reinforcement [13, 14] or an updated descending branch of the tensile stress-strain curve for concrete have been developed and implemented in FEM analyses [13, 15–20]. In addition, the so-called microscopic models based on the bond-slip mechanism and discrete cracking have been proposed by Floegl and Mang [21], Gupta and Maestrini [22], and Choi and Cheung [23].

Alternatively, several empirical models have been widely accepted by engineers in design for the control of deflections, involving determination of the effective moment of inertia ( $I_e$ ) for a cracked member under monotonic loading. Branson developed a well-known model [24], which has been adopted by the ACI Building Code [25]. Branson's equation gives a weighted average of the uncracked and cracked moments of inertia of the reinforced concrete cross-section at any load level, but it has been shown to overestimate the effective stiffness of lightly reinforced concrete beams and slabs [26]. In comparison with Branson's model, Bischoff suggested a weighted average of the uncracked and cracked flexibility of reinforced concrete cross-sections [27, 28]. Experiments carried out on reinforced slabs having reinforcement ratios ranging between 0.18% and 0.84% demonstrated that Bischoff's model is more accurate than Branson's model for lightly reinforced concrete members [26]. A statistical study that

employed data from nine experimental programs involving a total of 80 specimens showed a similar conclusion that the Branson's model overestimated the stiffness significantly for reinforcement ratios ranging between 0.4% and 0.8%[29]. Based on the local measurement and modeling of the steel reinforcement strains in the tensile zone, Xu et al. proposed an alternative empirical model, which provides a more conservative stiffness for lightly reinforced concrete beams[30].

Besides the effect of tension stiffening, Castel et al. [11, 31, 32] pointed out that the degradation of the moment of inertia and the irreversible deflection of the structural member due to cracking damage have to be accounted for in the serviceability analysis of existing cracked RC members. All the methods previously described are dedicated to the calculation of the deflection of structural members or the curvatures of cross-sections under monotonic increasing load up to failure [31]. As shown in Fig. 1, the path OABC is the monotonic load-deflection envelop obtained by performing a static load test beyond the cracking load  $P_{cr}$ . The stiffness of a reinforced concrete beam can be described by using the effective moment of inertia ( $I_e$ ) model [24, 28]. Owing to the the cracking damage, the unloading path in Fig. 1 is line BD, and the irreversible deflection is OD. When reloaded, the loading path is DB and the stiffness of the beam is proportional to the the average moment of inertia labelled  $I_a$  in Fig. 1 and discussed in Ref.[31]. The difference between  $I_a$  and  $I_e$  is significant and leads to relatively large differences in the calculated static deflection [11, 31, 32], as well as dissimilar dynamic properties, such as natural frequencies and responses to moving loads or vibrating machinery [33]. The question arises: *how much is the serviceability reliability reduced as a result of the cracking damage?* More recently, Murray reported that the effects of creep and shrinkage lead to time-dependent changes in the instantaneous stiffness[34]. These effects result in increments of both the time-dependent and instantaneous deflections, and might

Fig. 1. Typical overall response of RC-beams including a loading cycle

affect the long-term serviceability reliability of cracked reinforced concrete beams.

In this paper, serviceability issues related mainly to excessive deflection of structural elements (i.e. beams) are discussed. A quantitative analysis approach is proposed in order to evaluate the loss in the serviceability reliability due to historical cracking damage. In this approach, the effective moment of inertia is employed to simulate the pre-cracking loading up to  $P_{pre}$  and the following loading  $P$  when  $P > P_{pre}$ . And, the average moment of inertia is adopted to simulate the unloading from the pre-loading  $P_{pre}$  and the following loading  $P$  when  $P < P_{pre}$ . In the first part of the paper, the models of effective and average moment of inertia are introduced. Secondly, combining the sources of uncertainty for reinforced concrete beams and Monte Carlo simulation, a probability analysis approach for cracked reinforced concrete beams is presented. In this approach, experimental measured deflections and stochastic analysis results are compared in order to assess and compare the performance of the effective moment of inertia approach and the average moment of inertia approach. For both effective and average moment of inertia, the model error is calibrated by using experimental data from several sources. Finally, the influence of the historical cracking damage on both the short-term and long-term serviceability reliability is discussed by using numerical examples.

## 2. Deflection model

The total deflection  $\Delta_{G+Q}$  of a reinforced concrete member subjected to dead load and live loads can be expressed as

$$\Delta_{G+Q} = \Delta_G + \Delta_{Q,s} + \Delta_{Q,i} + \Delta_{cr} + \Delta_{sh} \quad (1)$$

where  $\Delta_G$  is the instantaneous deflection due to the dead load;  $\Delta_{Q,s}$  represents the instantaneous deflection due to the sustained live load;  $\Delta_{Q,i}$  stands for the instantaneous deflection due to the extraordinary live load;  $\Delta_{cr}$  is the time-dependent creep-induced deflections including the contributions of both dead load and sustained live load; and  $\Delta_{sh}$  is the time-dependent shrinkage-induced deflection.

To avoid the excessive deflection resulting in unintended load paths or damage to either structural or non-structural elements attached to the member, a limit is placed on the incremental deflection. The incremental deflection  $\Delta_{inc}$  is the sum of the time-dependent deflection due to the sustained loads and the instantaneous deflection due to the live load. It can be calculated as follows:

$$\Delta_{inc} = \Delta_{G+Q} - \Delta_G \quad (2)$$

The effect of creep and shrinkage on the total deformation of a reinforced concrete member consists of two parts. The first part is the time-dependent creep-induced and shrinkage-induced deflection ( $\Delta_{cr}$  and  $\Delta_{sh}$ ), which can be calculated by using the age-adjusted effective modulus method. The other part is the influence on the instantaneous stiffness of cracked reinforced concrete beams resulting in the increment of short-term deflection. Due to the creep and shrinkage, the bond between concrete and steel reinforcement is damaged leading to the reduction of tension stiffening effect. This results in a time-dependent increase in the so-called instantaneous deflections due to the sustained live load  $Q_s$  and the extraordinary live load  $Q_e$ .

In this paper, the instantaneous deflections of the reinforced concrete beam without prior cracking damage are calculated by using the effective moment of inertia  $I_e$  and the instantaneous deflections of the cracked member are calculated using both the effective moment of inertia and the average moment of inertia  $I_a$ .

### 3. Effective moment of inertia $I_e$

The deflection calculation procedure suggested by both Eurocode 2 [35] and the fib Model Code 2010[36] is considered to be an accurate and reliable model to calculate the shape of the instantaneous load-deformation response, especially for lightly reinforced members[26].

For a pure flexural member containing deformed bars, the effective moment of inertia proposed by Bischoff [27, 28] is determined as

$$I_e = \frac{I_{cr}}{1 - \eta \left(1 - \frac{I_{cr}}{I_{uncr}}\right) \left(\frac{M_{cr}}{M_a}\right)^2} \quad (3)$$

where  $M_{cr}$  and  $M_a$  are the cracking bending moment and the applied service bending moment respectively; and  $I_{cr}$  and  $I_{uncr}$  represent the moment of inertia of the fully cracked cross-section and the uncracked cross-section respectively;  $\eta$  is a coefficient accounting for both shrinkage-induced cracking and the reduction in tension stiffening with time, which can be calculated by

$$\eta = \begin{cases} 1.0 & \text{short-term} \\ 0.5 & \text{long-term} \end{cases} \quad (4)$$

### 4. Average moment of inertia $I_a$

When the load is increased above the cracking load primary bending cracks form at regular centres. When the steel reinforcement stress at the crack location reaches a threshold, interfacial microcracks form in the concrete between the primary cracks[37, 38]. These interfacial microcracks are often called cover-controlled cracks. Castel et

al. [37] proposed a bond damage criterion (i.e.  $\sigma_{s0} > \sigma_{s,ccc}$ ) as follows:

$$\sigma_{s,ccc}(f_{tc}) = \frac{Z_{nc}}{0.9Z_c} \left[ n + \frac{A_{tc,eff}}{A_s} \right] f_{tc} \quad (5)$$

where  $\sigma_{s,ccc}$  is the critical axial steel stress at the crack location leading to cover-controlled cracking;  $f_{tc}$  is the tensile strength of concrete;  $A_{tc,eff}$  is the effective area of active tensile concrete[32];  $A_s$  is the reinforcement area;  $n$  is the modular ratio of steel and concrete; and  $Z_c$  and  $Z_{nc}$  are the lever-arms of the internal forces on the cracked and uncracked cross sections respectively.

Accounting for the effects of both primary cracks and cover controlled cracks, a model for calculating the average moment of inertia  $I_a$  was developed by Castel et al.[11, 30–32] based on two assumptions: linear steel-concrete bond distribution assumption and constant bending moment assumption.

The linear distribution of the bond stress  $\tau(x)$  proposed by [39] as:

$$\tau(x) = \tau_{max} \frac{x}{l_{s,max}} \quad (6)$$

where  $\tau_{max}$  is the maximum shear stress close to the exact crack locations;  $x$  ( $0 < x < l_{s,max}$ ) is the distance from the cracks,  $l_{s,max}$  is the length over which slip between concrete and steel occurs as recommended by [36]. According to the definition of  $l_{s,max}$ , for the bond damage free beams, the strains of concrete  $\varepsilon_{tc,max}$  and tensile steel bars  $\varepsilon_{snc}$  are equal at  $x = l_{s,max}$  as:

$$\varepsilon_{tc,max} = \varepsilon_{snc} \quad (7)$$

A scalar variable  $D_{ccc}$  was introduced to evaluate the bond damage by calculating

the difference of the strain between the concrete and steel at  $x = l_{s,\max}$  in [32]:

$$\varepsilon_{tc,\max} = (1 - D_{ccc})\varepsilon_{snc} \quad (8)$$

When a beam is at the stabilized cracking stage, compared to the whole span of the beam,  $l_{s,\max}$  is small allowing to assume that the bending moment at all cross sections located along  $l_{s,\max}$  is constant as

$$M(x) = \text{constant}(0 \leq x \leq l_{s,\max}) \quad (9)$$

According to these assumptions, the distribution of the lever-arm of the internal forces  $Z(x)$  along  $l_{s,\max}$  can be calculated by[32]

$$Z(x) = \frac{Z_c Z_{nc}}{Z_c g(x) + [1 - g(x)] Z_{nc}} \quad (10)$$

where  $g(x)$  is a distribution function as

$$g(x) = 2\frac{x}{l_{s,\max}} - \left(\frac{x}{l_{s,\max}}\right)^2 \quad (11)$$

For a rectangular section, the depth to the neutral axis  $y_0(x)$  along  $l_{s,\max}$  can be derived as [32]

$$y_0(x) = 3[d - Z(x)] \quad (12)$$

where  $d$  is the effective depth of the tensile reinforcement.

By using Eq. (12), the moment of inertia distribution  $I(x)$  along the  $l_{s,\max}$  can be calculated. As recommended by [36], the average crack spacing is equal to  $1.5l_{s,\max}$ . Considering the symmetry between half cracks spacing, the average moment of inertia

$I_a$  between cracks can be calculated as follows:

$$I_a = \frac{\int_0^{0.75l_{s,\max}} I(x) dx}{0.75l_{s,\max}} \quad (13)$$

Restrained shrinkage can affect the stiffness of RC beams [40–42]. For cracked RC beams, restrained shrinkage induces tensile stress in concrete and encourages the formation and extension of microcracks at the steel-concrete interface over time resulting in the decay in tension stiffening. The effect of creep and shrinkage on the steel-concrete interfacial bond damage  $D_{cc}$  should be taken into account [34].

More detail of Castel et al. model can be seen in Ref.[30, 32, 34].

## 5. Creep and shrinkage model

Several creep and shrinkage models, such as ACI 209 model [25], CEB-FIP model[36], B3 model [43] , GL2000 model [44, 45] are available. In the present study, MC90 model is selected to account for creep and shrinkage of concrete [46].

## 6. Uncertainty sources

The uncertainties affecting the stiffness of a beam are related to either the material properties, the applied loadings, and the geometry of the cross-section.

### 6.1. Uncertainty of material properties

For the concrete, the parameters that possess a random nature include the compressive strength ( $f_c$ ), the tensile strength ( $f_{tc}$ ), and the elastic modulus ( $E_c$ ). It is generally accepted that there is a strong correlation between  $f_c$ ,  $f_{tc}$ , and  $E_c$ [47, 48]. Correlation between the elastic modulus and the compressive strength of the concrete has been used by Keitel and Osburg[49] in uncertainty analysis relating to creep

and shrinkage by mean of a direct correlation coefficient. An alternative approach is adopted in the present work. According to the JCSS Probabilistic Model Code and fib Model Code 2010, by multiplying the tensile strength and elastic modulus by random variables, the stochastic correlation between tensile strength  $f_{tc}$ , elastic modulus of concrete  $E_{c0}$  and the mean compressive strength  $f_c$  at age of 28 days is defined as[36, 50]

$$f_c = \gamma_1 f_{cm} (\text{MPa}) \quad (14a)$$

$$f_{tc} = \gamma_2 0.3 f_c^{2/3} (\text{MPa}) \quad (14b)$$

$$E_{c0} = \gamma_3 21.5 \times 10^3 \left(\frac{f_c}{10}\right)^{1/3} (\text{MPa}) \quad (14c)$$

in which,  $\gamma_1$ ,  $\gamma_2$ , and  $\gamma_3$  are treated as independent normal random variables [50].

The modulus of elasticity of concrete at age  $t$  may be estimated from

$$E_c(t) = E_{c0} \sqrt{\exp \left[ s \left( 1 - \sqrt{28/t} \right) \right]} \quad (15)$$

Since current creep and shrinkage models are generally based on the mean value of experimental results, model uncertainty should be a concern [47]. The stochastic model of time-dependent strain can be calculated by [51]

$$\varepsilon(t) = [\gamma_4 J(t, t_0)] \sigma(t_0) + \int_{t_0}^t [\gamma_4 J(t, \tau)] d\sigma(\tau) + \gamma_5 [\varepsilon_{sh}(t - t_s) - \varepsilon_{sh}(t_0 - t_s)] \quad (16)$$

in which the time-dependent strain  $\varepsilon(t)$  consists of short-term strain caused by the loading at age  $t_0$  and the long-term strain caused by creep and shrinkage at age  $t$ ; and,  $\gamma_4$  and  $\gamma_5$  are assumed to be normal random variables, related to the uncertainty of the creep and shrinkage models [43].

Fig. 2. Time histories of typical live loads

For reinforcement, the probability distribution of the yield strength is a normal distribution with the mean value of  $f_{yn} + 2 \times 30\text{MPa}$ , and standard deviation of  $30\text{MPa}$  [50], where  $f_{yn}$  is its nominal value. The elastic modulus is considered as  $\gamma_6 E_{sm}$ , where  $E_{sm}$  is the mean value of elastic modulus of the reinforcing steel bars.

### 6.2. Uncertainty of cross-section

In this paper, the randomness of cross-section is also considered in this paper. The parameters of cross-section are treated as normal random variables, including the overall depth of the cross-section ( $\gamma_7 h_m$ ), the width of the cross-section ( $\gamma_8 b_m$ ), the effective depth of cross-section ( $\gamma_9 d_m$ ), and the area of tensile reinforcement ( $\gamma_{10} A_{sm}$ ).

### 6.3. Uncertainty of loads

Typical loads applied to structures include dead load and live loads, that can be simulated by using recommended statistical models. The dead load  $G$  is treated as a normal random variable with mean of 1.05 times its nominal value  $G_n$  with a coefficient of variation of 0.10 [52, 53]. The live loads consist of the sustained live load  $Q_s$  and the extraordinary live load  $Q_e$  as shown in Fig. 2. The sustained live load is modeled by a Gamma distribution with mean of  $0.30Q_n$  ( $Q_n$  denotes a nominal value of live load) with a coefficient of variation of 0.60[53]. The mean duration of the sustained live loads is often assumed to be eight years, corresponding to the average period between tenant changes in office building [54]. Extraordinary live load is also modeled by using a Gamma distribution with an annual mean of  $0.19Q_n$  and a coefficient of variation of 0.66 [53].

The statistical parameters of the random variables are summarized in Table 1.

Table 1. Statistical Properties of Random variables

Variables	Distribution type	Mean	COV	Uncertainty sources
$\gamma_1$	Log-normal	1.00	0.06	$f_c$ [50]
$\gamma_2$	Log-normal	1.00	0.30	model of $f_{tc}$ [50]
$\gamma_3$	Log-normal	1.00	0.15	model of $E_{c0}$ [50]
$\gamma_4$	Normal	1.00	0.32	model of creep [45]
$\gamma_5$	Normal	1.00	0.37	model of shrinkage [45]
$\gamma_6$	Normal	1.00	0.033	$E_s$ [53]
$\gamma_7$	Normal	1.00	0.045	$h$ [55]
$\gamma_8$	Normal	1.00	0.045	$b$ [55]
$\gamma_9$	Normal	1.00	0.05	$d$ [55]
$\gamma_{10}$	Normal	1.00	0.02	$A_s$ [50]
$G$	Normal	$1.05G_n$	0.10	dead load[53]
$Q_s$	Gamma	0.30	0.60	sustained live load[53]
$Q_e$	Gamma	0.19	0.66	extraordinary live load[53]
$f_y$ (MPa)	Normal	$f_{yn} + 60$	std = 30	$f_y$ [50]

## 7. Experiment, stochastic analysis, and model error of average moment of inertia

### 7.1. Experiment program

In order to investigate the randomness of the average moment of inertia for cracked RC beams, results of the analyses of eleven beams tested as part of this study are reported in this paper (named as B1 to B11). Two different concrete mixes were used, with average compressive strengths of 38 MPa and 46 MPa after 28 days, respectively. The mechanical characteristics of the concrete (mean compressive strength  $f_{cm}$ , mean tensile strength  $f_{tcm}$ , mean elastic modulus  $E_{cm}$ ) are listed in Table 2. The main steel reinforcement consisted of Australian Class N deformed bars of either 16 mm or 20 mm diameter. The reinforcement ratios  $\rho$  are shown in Table 2. The characteristic yield strength of the reinforcement was 500 MPa. The average yield stress of the reinforcing bars was 520.00 MPa (standard deviation was 5.43 MPa). The beams

Fig. 3. Layout of the reinforcement and loading arrangement (mm)

(a)  
Short-term  
term

Fig. 4. Setup of (a) short-term and (b) long-term loading

were demolded 24h after casting and stored under various conditions until the load tests commenced at age 28 days. B3 and B4 were moist cured for only seven days and then stored in the laboratory, while the other beams were stored in a high moisture environment until testing.

As shown in Fig. 3, all beams were 3500 mm long, with a 3300 mm span between simple supports and with a uniform 400×300 mm cross-section. The cover of the main reinforcing bars was 35 mm. The effective depth of the tensile reinforcement  $d$  was either 355 or 357 mm. At 28 days after casting, all beams were tested in 4-point bending for the precracking load tests as shown in Fig. 4(a). Each beam was subjected to 10 loading and unloading cycles in order to assess the instantaneous stiffness after cracking and the permanent residual deflection after unloading. The beams were then subjected to a sustained load for a period of six months by using an appropriate spring loading device to ensure that the load remained constant for the duration of the test as shown in Fig. 4(b). After six months, the beams were subjected to the same cycles of unloading/reloading to again measure the instantaneous stiffness and assess any changes due to time-dependent effects. Table 3 shows the values of maximum applied moment  $M_a$  (including the self-weight) for all beams. During the test, the deflection at the mid-span of the beam was measured by using LVDT. For each beam, after unloading, the crack distribution of each side (i.e. south side and north side) was recorded as shown in Fig. 5 for B1 as an example.

Table 2. Concrete and reinforcement properties of beams

Beams	$f_{cm}$ (MPa)	$f_{tcm}$ (MPa)	$E_{cm}$ (GPa)	$d_b$ (mm)	$A_{sm}$ (mm <sup>2</sup> )	$\rho$
B1	46	3.5	33	3 $\phi$ 16	603	0.56%
B2	46	3.5	33	3 $\phi$ 16	603	0.56%
B3	46	3.5	33	3 $\phi$ 16	603	0.56%
B4	46	3.5	33	3 $\phi$ 16	603	0.56%
B5	38	3.8	35	3 $\phi$ 16	603	0.56%
B6	46	3.5	33	3 $\phi$ 16	603	0.56%
B7	38	3.8	35	2 $\phi$ 16+ $\phi$ 20	716	0.67%
B8	38	3.8	35	3 $\phi$ 16	603	0.56%
B9	38	3.8	35	3 $\phi$ 16	603	0.56%
B10	38	3.8	35	3 $\phi$ 20	942	0.88%
B11	38	3.8	35	3 $\phi$ 20	942	0.88%

Fig. 5. Actual crack distribution of beam B1

Table 3. Maximum applied moment, steel stress and the damage criteria

Beams	$M_a$ (kN · m)	$\sigma_{s0}$ (MPa)	$D_{ccc}$	$\sigma_{s,ccc}$ (MPa)
B1	40.2	201	0.00	230
B2	39.3	197	0.00	230
B3	35.6	179	0.00	230
B4	39.6	199	0.00	230
B5	44.2	222	0.00	250
B6	51.4	258	0.97	230
B7	57.8	246	0.92	215
B8	57.8	290	0.98	250
B9	69.9	351	0.98	250
B10	60.2	197	0.80	168
B11	45.0	147	0.00	168

(600)  
~~1134~~

Fig. 6. Experimental load-deflection responses(B1 to B4)

Fig. 7. Probability distribution of average moment of inertia ( $\bar{I}_a = 6.16 \times 10^{-4} \text{m}^4$ , COV=17%)

### 7.2. Stochastic analysis of short-term average moment inertia of B1 to B4

As shown in Table 2 and 3, Beam B1 to B4 were cast with the same cross-section, material, and loading arrangement. These beams were loaded without exceeding the steel stress threshold (Eq. 5) leading to interfacial microcracks (i.e. steel-concrete bond damage between the primary cracks). The differences between these four beams are the storage environments and the applied loading. The experimental load-deflection responses of B1 to B4 are shown in Fig. 6. Finally, all beams were loaded up to failure. The failure loads  $P_u$  are also plotted in Fig. 6. According to the load-deflection response, the unloading/reloading experimental stiffness and residual deflection after unloading of the cracked beam can be obtained. In the uncracked zone of the beam span near the supports, the gross moment of inertia ( $I_g$ ) can be used, whereas the average moment of inertia ( $I_a$ ) is assembled to the cracked zone. In this way, the residual deflection of the beam can be calculated by taking the applied preloading  $P_{pre}$  into account. The experimental average moment of inertia can be assessed by minimizing the difference between measured and calculated residual deflection. The results are presented in Fig. 7.

The steel stresses at the cracked section  $\sigma_{s0}$  and the values of  $D_{ccc}$  as well as  $\sigma_{s,ccc}$  of each beam are shown in Table 3. According to the cover-control cracking criteria (Eq. 5), B1 to B4 should not present any concrete damage at the interface with the steel bars and hence  $I_a$  is expected to be the same for each of the beams B1 to B4.

However, due to the natural uncertainties of RC structures, the experimental  $I_a$  of each beam is different as shown in Fig. 7. Using Monte Carlo Simulation (MCS), the probability characteristics of  $I_a$  can be calculated, and are plotted in Fig. 7. The results show that the probability density function is similar to a normal distribution, the mean value  $\bar{I}_a$  is  $6.16 \times 10^{-4} \text{ m}^4$  with the COV of 17%, and the lower and upper fractiles (2.28% and 97.72%) are  $4.10 \times 10^{-4} \text{ m}^4$  and  $8.1 \times 10^{-4} \text{ m}^4$  respectively. All the experimental values of  $I_a$  fall in the probability interval (2.28% to 97.72%) in the high probability density zone. The comparison between experimental results and stochastic analysis shows the precision of the average moment of inertia model.

### 7.3. Calibration of model error of moment of inertia $\gamma_{11}$

The short-term experimental data from the tests carried out on eleven beams at UNSW Australia as well as test results from two additional sources from the literatures[56–58] are used to calibrate a probabilistic distribution for the model error of the average moment of inertia  $I_a$ . The actual material properties (e.g. the mean value of elastic modulus of concrete and steel  $E_{cm}$  and  $E_{sm}$ ), section dimensions, ratios of tensile reinforcement and the loading arrangement can be measured in the laboratory. Using cyclic load-deflection tests results, the experimental value of  $I_a$  for each beam was assessed as mentioned in Section 7.2. Fig. 8(a) illustrates the relationship between the predicted and test values of the normalized average moment of inertia  $I_a/I_g$ . Results presented in Fig. 8(a) show that the Castel et al. model is reasonably able to predict the average moment of inertia for cracked reinforced concrete beams. It is assumed that in the collected experimental data, the mechanical properties as well as cross-section dimensions were accurately measured. Hence, the only uncertainty is that associated with the analytical model[59]. The mean value of short-term model error  $\bar{\gamma}_{11}$  is 1.02 with the COV of 9.6 %. Similarly, the model uncertainty of the

(b)  
 Long-  
 term  
 av-  
 er-  
 age  
 mo-  
 ment  
 of  
 in-  
 er-  
 tia

Fig. 8. Scatter of experimental and analytical values for normalized average moment of inertia

time-dependent effects of creep and shrinkage on the average moment of inertia is calibrated by using the tested data reported by Murray [34]. The mean value of long-term model error  $\bar{\gamma}_{11}$  is 1.00 with the COV of 12.1 % (Fig. 8(b)). Due to the lack of experimental data, the probabilistic distribution of the model error is assumed to be a normal distribution. In further, more experiments are required in order to improve the calibration of the model error of the average moment of inertia and to cover a wider range of material strengths, reinforcement ratios, and specimen sizes.

In order to cover more area of the applications of effective moment of inertia, a total of 505 observations of Gilbert[60] and Gribniak [29, 61] are adopted to calibrate the model error of the effective moment of inertia. In Ref.[60], Gilbert reported experimental results obtained on a total of eleven lightly reinforced concrete beams (slabs). The deflections of the beams (slabs) were measured for different loading values after cracking:  $1.1M_{cr}$ ,  $1.2 M_{cr}$  and  $1.3M_{cr}$ . In Ref.[29, 61], a total of eight lightly reinforced concrete beams were tested under a four-point loading scheme. The measured curvatures in each load step were reported. Similar to the model error of the average moment of inertia, the ratio between experimental and predicted results

Fig. 9. Histogram and probability density of the model error of the effective moment of inertia

calculated by using the effective moment of inertia is defined as the model error  $\gamma_{11}$ . The histogram and probability density of the model error  $\gamma_{11}$  are plotted in Fig. 9. It can be seen that the model error for effective moment of inertia can be treated as a lognormal random variable with the mean value of 0.96, and with the COV of 0.20.

It is noted that the calibration of model errors of the moment of inertia is based on the short-term experiments. The uncertainty relating to creep and shrinkage effects is taken into account by using  $\gamma_4$ ,  $\gamma_5$ , and Eq. (16) as mentioned in Section 6.1.

## 8. Serviceability reliability analysis

### 8.1. Determined deflection analysis for cracked concrete beams

For the in-service response, the stress-strain relationship for concrete in compression is taken to be linear elastic. For pure bending problems, assembling the appropriate moment of inertia for cracked reinforced concrete beams, a static analysis can be performed via the finite element method to calculate the deflections of the beams. As shown in Fig. 10, for the case of four points loading, the length of the cracked zone of the beam depends on the relative values of the cracking moment  $M_{cr}$  and the maximum applied moment  $M_a$ . The moments of inertia adopted for the uncracked zone near the supports is the gross moment of inertia  $I_g$ . In the cracked zone, either the effective moment of inertia  $I_e$  or the average moment of inertia  $I_a$  is used in order to compare the performance of both approaches in the serviceability reliability analysis.

Fig. 10. Assembling the moment of inertia for the overall beam response calculation

### 8.2. Serviceability requirement

The serviceability requirements can include the beam deflection, the crack width, the level of vibration, the degree of spalling, etc. In this paper, the serviceability issues relating to excessive deflection are discussed.

Allowable deflection limits for use in structural design are specified in most standards or codes of practice and depend on the function of the beam or slab. As shown in Table 4, allowable deflection limits obtained from ACI 318-14[25] for elements in buildings are approximately equivalent to those from fib Model Code 2010 and Eurocode 2[35, 36], whereas the requirements for bridges from AASHTO (2002)[62] are much stricter.

Table 4. Suggested Deflection Limits for Structural Elements

Code	Limitation	Condition
ACI 318-14	$L/240$	Supporting or attached to non structural elements which are not likely to be damaged by large deflection
	$L/480$	Supporting or attached to non structural elements which are likely to be damaged by large deflection
<i>fib</i> Model Code 2010	$L/250$	quasi-permanent loads could impair the appearance and general utility
/ Eurocode 2	$L/500$	quasi-permanent loads could damage adjacent parts of the structure
AASHTO LRFD Bridge	$L/800$	General vehicular load
Design Specifications	$L/1000$	Vehicular and/or pedestrian load

In this paper, the ACI 318-14 requirements are selected as an example to show the effects of cracking damage of existing reinforced concrete beams on the serviceability reliability. According to ACI 318-14, two different deflection limits must be satisfied

for slabs and beams supporting (or attached to) nonstructural elements. For the attached non-structural elements which are not likely be damaged by large incremental deflections  $\Delta_{\text{inc}}$ , the sum of the time-dependent deflection due to sustained loads and the immediate deflection due to live load should not exceed  $L/240$  ( $\Delta_1$ ), where  $L$  is the span of the slab or beam. The corresponding probability of serviceability failure  $P_{f_1}$  is given by

$$P_{f_1} = P_r(\Delta_1 - \Delta_{\text{inc}} < 0) \quad (17)$$

where  $P_r(\cdot)$  is the probability of the even (e.g.  $\Delta_1 - \Delta_{\text{inc}} < 0$  in Eq. (17)).

For the attached nonstructural elements which are likely be damaged by large deflection,  $\Delta_{\text{inc}}$  should not exceed  $L/480$  ( $\Delta_2$ ). The corresponding probability of serviceability failure  $P_{f_2}$  is given by

$$P_{f_2} = P_r(\Delta_2 - \Delta_{\text{inc}} < 0) \quad (18)$$

### 8.3. Serviceability reliability analysis methodology

Monte Carlo simulation (MCS) is adopted here to calculate the serviceability reliability of cracked reinforced concrete beams. The accuracy of MCS depends on the sample sizes and the value of the probability of failure (the smaller the probability of failure, the larger the sample size required to ensure the same accuracy)[53]. Considering that the target reliability index  $\beta$  for existing structures are 3.0 (reference period 1 year) and 1.5 (reference period 50 years) for serviceability limited states verification in fib Model Code [36], a total of  $M = 10^6$  samplings is large enough to satisfy the sampling requirements.

For an intact reinforced concrete beam, the serviceability reliability can be calculated by using the effective moment of inertia, and the calculation steps are as

follows:

- 1: Sampling the random variables of structure and dead load to model a beam;
- 2: Sampling the sustained and extraordinary live loads in the reference period;
- 3: Calculating the deflection by using monotonic loading stiffness (Eq. (3)) dependent on the maximum live loads combination;
- 4: Increasing by one for failure counter ( $m$ ), if the deflection is larger than the limit.

For an cracked reinforced concrete beam damaged by a historical load ( $P_{pre}$ ), the deduction of stiffness and the historical irreversible deflection have to be taken into account by using the average moment of inertia. For every sampling in MCS, the analysis is carried out as follows:

- 1: Sampling the random variables of structure and dead load to model a beam;
- 2: Calculating the instantaneous deflection caused by a historical loading resulting in cracking of the beam by Eq. (3);
- 3: Calculating the irreversible deflection and average stiffness by Eq. (13)
- 4: Sampling the sustained and extraordinary live loads in the reference period;
- 5: if the maximum combined live load is less than the historical loading, go to 7;
- 6: Calculating the deflection by using the monotonic loading stiffness (Eq. (3)) dependent on the maximum combined live load; go to 9;

- 7: Calculating the deflection caused by sampling live load with reloading stiffness using by Eq. (13);
- 8: Calculating the total deflection by summing the irreversible and reloading deflections;
- 9: Increasing by one for failure counter ( $m$ ), if the total deflection is larger than the deflection limit.

The failure probability for the serviceability limit state of cracked reinforced concrete beams incorporating cracking damage can be obtained by

$$P_f = \frac{m}{M} \quad (19)$$

The reliability index is

$$\beta = -\Phi^{-1}(P_f) \quad (20)$$

## 9. Numerical examples

The reinforced concrete beam B1 is selected as a study case. Both dead load and live loads are assumed to be uniform loading. The nominal value of the dead load  $G_n$  is assumed to be 24kN/m, incorporating other dead loads from the attached elements (e.g. the self-weight of the concrete floor with thickness of 0.14 m and with influence width of 6 m). Three levels of historical damaging loads ( $P_1 = 20\text{kN}$ ,  $P_2 = 60\text{kN}$ , and  $P_3 = 100\text{kN}$ ) inducing cracking are applied to the beam. The sum of applied bending moment due to the dead load and the damaging load are about 40%, 60%, and 80% of the yielding bending moment in each level, respectively.

(a)  
  
 1234

Fig. 11. Probability density function of the short-term deflections at the mid-span

(b)  
  
 $\beta_2$

Fig. 12. Short-term serviceability reliability index vs.  $Q_n/G_n$  ( $\beta_1$  and  $\beta_2$  are the reliabilities related to deflection limitation  $\Delta_1$  and  $\Delta_2$  respectively)

### 9.1. Short-term deflection

Using the MCS, the probability density distributions of the short-term deflection at mid-span with the increment of the nominal value of live load was calculated for each level of historical load. The corresponding short-term serviceability reliability index was analyzed as well. The results with and without considering historical cracking damage are plotted in Fig. 11 and Fig. 12 respectively. The influence of the historical damaging load on the probability density distribution of the deflection significantly due to the irreversible deflection and the deduction of the stiffness, when  $Q_n/G_n = 1$  and  $Q_n/G_n = 2$ , is shown in Fig. 11(a) and 11(b). However, as the increment of the nominal value of the live load, the difference decreases as shown in Fig. 11(d). The reliability index is affected by the historical damage as well. However, it is interesting that the reliability index of the beam subjected to the first load level ( $P_1$ ) is the same with the undamaged beam, although the probability density distribution is different, as shown in Fig. 11. These phenomena can be explained by using Fig. 13.

In Fig. 13(a), when the applied live load  $P$  is larger than the historical damaging load  $P_{pre}$ , the loading path returns to the monotonic path (OBC) as shown in Fig. 13(a). In this scenario, there is no influence of the historical damage on the live

(b)  
 $H_a >$   
 $H_{pre}$

Fig. 13. Typical overall response of RC-beams vs deflection limitation

load deflection. However, if the applied live load  $P$  is less than the historical load  $P_{pre}$  (Fig. 13(b)), the loading path is ODE, and the deflection response ( $\Delta$ ) due to the applied live load should be calculated by

$$\Delta = \Delta_{perm,cr} + \Delta_{inst} \quad (21)$$

where  $\Delta_{inst}$  is the instantaneous deflection of the cracked beam under loading and unloading cycles. For the light damage induced by the first loading level  $P_1$ , the live load  $P$  is always larger than the historical load and less influence is observed on the short-term serviceability reliability as shown in Fig. 12. For heavier damage (e.g.  $P_{pre} = P_2$  or  $P_3$ ), with increases in the nominal value of live load, the influence of the historical damage loading on both the probability density distribution of the deflection and the serviceability reliability index of the damaged beam decreases as shown in Fig. 11 and 12.

The effect of cracking on the serviceability reliability index also depends on the deflection limit selected.  $P_a$  is the critical load related to the deflection limit for the serviceability limit state in the monotonic load-deflection envelop curve as shown in Fig. 13(a) for one of the random samplings. When the historical loading  $P_{pre}$  is lower than  $P_a$ , all of the applied live loads  $P$  causing serviceability failure are larger than the historical damaging load  $P_{pre}$ . Hence, although historical damage affects the probability density distribution of the deflection as shown in Fig. 11 ( $P_{pre} = P_1$ ), no influence is observed on the serviceability reliability. When the historical loading

is larger than  $P_a$ , the deflection due to an applied load  $P$ , lower than  $P_a$ , should be calculated using Eq. (21). The failure criterion should be modified as

$$P > P_b \quad (22)$$

in which  $P_b$  is the critical load related to the deflection limit for the serviceability limit state in the cycle loading path (DE). Obviously, the risk of failure will increase when  $P_b < P_a$ . In the stochastic analysis, both  $P_a$  and  $P_b$  are random variables and, even when the mean value of deflection induced by historical loading is less than the deflection limitation, there is still a remarkable influence of the cracked damage on the serviceability reliability. The criterion can be defined as follows:

$$P_r(P_{pre} > P_a) > 0 \quad (23)$$

### 9.2. Long-term deflection

As shown in Fig. 14, the beam considered here was loaded 28 days after concrete placement with the dead load, and was then occupied by the tenants and subjected to the sustained live load 180 days after concrete placement. The beam is assumed to have eight different tenants. And, the average tenancy duration is assumed to be eight years [54, 63]. Thus, the expected design life of the beam is 64.5 years. Under the dead load and the sustained live load, the long-term effects of creep and shrinkage were calculated. During the tenant period, the extraordinary live load was also applied to the beam. This type of load is transient in nature, and is not taken into account in the creep analysis.

In this paper, two damaged scenarios have been considered: the historical damaging load was applied 180 days (case C1) and 3000 days (case C2) after concrete

Fig. 14. The development of the total deflection of the beam including the time-dependent effects

$$\frac{(\Delta_0)}{HE_3}$$

Fig. 15. Long-term serviceability reliability index vs.  $Q_n/G_n$

placement, respectively. The long-term serviceability reliability index  $\beta_2$  relating to the deflection limitation  $\Delta_2$  was calculated. The results are plotted in Fig. 15. Similar to the short-term serviceability reliability analysis, the historical damage leads to a decrement in the long-term serviceability reliability. However, the results are different from those of the short-term analysis in that the reliability index in the damaged beam is lower than that of the undamaged beam, even when the historical load  $P_{pre}$  is only 20kN. The reduction of the overall stiffness due to the historical cracking damage influences both the immediate deflection caused by the extraordinary live load and the time-dependent deflection due to the dead load and sustained live load. Although the extraordinary live load is larger than the historical load  $P_1$ , with the result that the instantaneous loading path returns to the monotonic loading as show in Fig. 13(a), the damage to the stiffness affects the time-dependent deflection leading to the reduction of the long-term serviceability reliability. The age of concrete when the historical damage load was applied influences the long-term serviceability reliability. In this example, the long-term serviceability reliability index for the case C1 was considerable lower than the reliability index for the case C2, as shown in Fig. 15. According to MC 90 model, the mean value of creep coefficients at the age of 180 and 3000 days are 63% and 95% of the mean value of the final creep coefficient, respectively. Thus, the cracking damage applied at the age of 3000 days of concrete has little influence on the creep effect.

## 10. Conclusion

In this paper, an existing model allowing calculation of the average moment of inertia of RC beams during cycles of loading and unloading is modified to take into account the effect of historical cracking damage on the serviceability reliability of RC members. The suitability of the average moment of inertia model for reliability analysis is verified by considering experimental tests on a total of eleven reinforced concrete beams. The model errors associated with both the effective and the average moment of inertia are calibrated using the experimental data. Combining the sources of uncertainty of RC-members and MCS, a quantitative analysis approach is presented to evaluate the loss in serviceability reliability due to the historical cracking damage for the reinforced concrete beam.

By using the proposed approach, both short-term and long-term serviceability reliability of a cracked reinforced concrete beam was analyzed. The results confirm that the effect of historical cracking damage on short-term serviceability reliability should be taken into account, when the deflection induced by historical loading is larger than the deflection limitation. In such a scenario, neglecting the historical cracking damage leads to overestimation of the serviceability reliability of cracked RC-members. Light historical damage (e.g.  $P_{\text{pre}} = P_1$ , in this case) has no influence on the short-term serviceability reliability, although it affects the probability density distribution of the deflection of the beam. However, even when the historical damage is light, the long-term serviceability reliability index is decreased as the cracking damage affects the time-dependent deflection. Additionally, the later the damaging load is applied to the reinforced concrete beam, the less influence the cracking damage has on the long-term serviceability reliability.

The proposed method can be used to quantitatively evaluate the residual service-

ability reliability of existing cracked damage reinforced concrete beams.

## 11. Acknowledgement

Authors are very grateful for the funding from National Key Research and Development Program of China with Grant No.2016YFB1200401 and 2016YFC0802205, the projects 51308468 and 51378432 supported by National Natural Science Foundation of China, the projects DP110103028 and DP140100529 supported by the Australian Research Council, and Research and Development Project (2014-02-015) supported by Department of Communications of Guangdong Province. The first author wishes to thank the Key Laboratory of High-speed Railway Engineering, Ministry of Education, Southwest Jiaotong University, People's Republic of China, for its support.

## 12. References

- [1] B. V. Vliet, I. T. Vrouwenvelder, Reliability in the performance-based concept of fib model code 2010, *Structural Concrete* 14 (4) (2013) 309–3019.
- [2] D. M. Frangopol, Y. Ide, E. Spacone, I. Iwaki, A new look at reliability of reinforced concrete columns, *Structural Safety* 18 (2) (1996) 123–150.
- [3] D. Val, F. Bljoger, D. Yankelevsky, Reliability evaluation in nonlinear analysis of reinforced concrete structures, *Structural Safety* 19 (2) (1997) 203–217.
- [4] R. E. Melchers, *Structural reliability analysis and prediction*, John Wiley & Son Ltd, 1999.

- [5] R. Soares, A. Mohamed, W. S. Venturini, M. Lemaire, Reliability analysis of non-linear reinforced concrete frames using the response surface method, *Reliability Engineering & System Safety* 75 (1) (2002) 1–16.
- [6] R. A. Neves, A. Chateauneuf, W. S. Venturini, M. Lemaire, Reliability analysis of reinforced concrete grids with nonlinear material behavior, *Reliability Engineering & System Safety* 91 (6) (2006) 735–744.
- [7] T. Xiang, R. Zhao, Reliability evaluation of chloride diffusion in fatigue damaged concrete, *Engineering structures* 29 (7) (2007) 1539–1547.
- [8] T. Xu, T. Xiang, Y. Zhan, R. Zhao, Reliability analysis of circular concrete-filled steel tube with material and geometrical nonlinearity, *Journal of Modern Transportation* 20 (3) (2012) 138–147.
- [9] Y. Jiang, G. Sun, Y. He, M. Beer, J. Zhang, A nonlinear model of failure function for reliability analysis of rc frame columns with tension failure, *Engineering Structures* 98 (2015) 74–80.
- [10] N. B. Hossain, M. G. Stewart, Probabilistic models of damaging deflections for floor elements, *Journal of performance of constructed facilities* 15 (4) (2001) 135–140.
- [11] A. Castel, T. Vidal, R. François, Finite-element modeling to calculate the overall stiffness of cracked reinforced concrete beams, *Journal of Structural Engineering* 138 (7) (2012) 889–898.
- [12] V. Gribniak, H. A. Mang, R. Kupliauskas, G. Kaklauskas, Stochastic tension-stiffening approach for the solution of serviceability problems in reinforced con-

- crete: Constitutive modeling, *Computer-Aided Civil and Infrastructure Engineering* 30 (9) (2015) 684–702.
- [13] R. I. Gilbert, R. F. Warner, Tension stiffening in reinforced concrete slabs, *Journal of the structural division* 104 (12) (1978) 1885–1900.
- [14] C.-K. Choi, S.-H. Cheung, A simplified model for predicting the shear response of reinforced concrete membranes, *Thin-walled structures* 19 (1) (1994) 37–60.
- [15] A. Scanlon, D. W. Murray, Time-dependent reinforced concrete slab deflections, *Journal of the Structural Division* 100 (9) (1974) 1911–1924.
- [16] F. J. Vecchio, M. P. Collins, The modified compression-field theory for reinforced concrete elements subjected to shear, in: *ACI Journal Proceedings*, Vol. 83, ACI, 1986, pp. 219–231.
- [17] B. Massicotte, A. E. Elwi, J. G. MacGregor, Tension-stiffening model for planar reinforced concrete members, *Journal of Structural Engineering* 116 (11) (1990) 3039–3058.
- [18] R. S. Stramandinoli, H. L. La Rovere, An efficient tension-stiffening model for nonlinear analysis of reinforced concrete members, *Engineering Structures* 30 (7) (2008) 2069–2080.
- [19] G. Kaklauskas, J. Ghaboussi, Stress-strain relations for cracked tensile concrete from rc beam tests, *Journal of Structural Engineering* 127 (1) (2001) 64–73.
- [20] L. Torres, F. Lopez-Almansa, L. M. Bozzo, Tension-stiffening model for cracked flexural concrete members, *Journal of Structural Engineering* 130 (8) (2004) 1242–1251.

- [21] H. Floegl, H. A. Mang, Tension stiffening concept based on bond slip, *Journal of the Structural Division* 108 (12) (1982) 2681–2701.
- [22] A. K. Gupta, S. R. Maestrini, Tension-stiffness model for reinforced concrete bars, *Journal of Structural Engineering* 116 (3) (1990) 769–790.
- [23] C.-K. Choi, S.-H. Cheung, Tension stiffening model for planar reinforced concrete members, *Computers & structures* 59 (1) (1996) 179–190.
- [24] D. E. Branson, Instantaneous and time-dependent deflections of simple and continuous reinforced concrete beams, HPR Report No.7, Alabama Highway Dept., Bureau of Public Roads (1963).
- [25] ACI-318, Building code requirements for structural concrete (aci 318-14) and commentary on building code requirement for structural concrete (aci318r-14), American Concrete Institute, 2014.
- [26] R. I. Gilbert, Tension stiffening in lightly reinforced concrete slabs, *Journal of structural engineering* 133 (6) (2007) 899–903.
- [27] P. H. Bischoff, Reevaluation of deflection prediction for concrete beams reinforced with steel and fiber reinforced polymer bars, *Journal of Structural Engineering* 131 (5) (2005) 752–767.
- [28] P. H. Bischoff, Rational model for calculating deflection of reinforced concrete beams and slabs, *Canadian Journal of Civil Engineering* 34 (8) (2007) 992–1002.
- [29] V. Gribniak, V. Cervenka, G. Kaklauskas, Deflection prediction of reinforced concrete beams by design codes and computer simulation, *Engineering Structures* 56 (6) (2013) 2175–2186.

- [30] T. Xu, A. Castel, R. I. Gilbert, A. Murray, Modeling the tensile steel reinforcement strain in rc-beams subjected to cycles of loading and unloading 126 (2016) 92–105.
- [31] A. Castel, R. François, Calculation of the overall stiffness and irreversible deflection of cracked reinforced concrete beams, *Advances in Structural Engineering* 16 (12) (2013) 2035–2042.
- [32] A. Castel, R. I. Gilbert, G. Ranzi, Instantaneous stiffness of cracked reinforced concrete including steel-concrete interface damage and long-term effects, *Journal of Structural Engineering* 140 (6) (2014) 1299–1328.
- [33] T. Xu, A. Castel, Modeling the dynamic stiffness of cracked reinforced concrete beams under low-amplitude vibration loads, *Journal of Sound and Vibration* 368 (2016) 135–147.
- [34] A. Murray, A. Castel, R. I. Gilbert, C. Zhen-Tian, Time-dependent changes in the instantaneous stiffness of reinforced concrete beams, *Engineering Structures* 126 (2016) 641–651.
- [35] European Committee for Standardization (CEN), Eurocode 2: Design of Concrete Structures: Part 1-1: General Rules and Rules for Buildings, prEN 1992-1-1:2003, European Prestandard, Brussels, Belgium, 2003.
- [36] CEB-FIB Model, CEB-FIB Model Code 2010–Final draft, 2010.
- [37] A. Castel, R. François, Modeling of steel and concrete strains between primary cracks for the prediction of cover-controlled cracking in rc-beams, *Engineering Structures* 33 (12) (2011) 3668–3675.

- [38] H. Wu, R. Gilbert, Modeling short-term tension stiffening in reinforced concrete prisms using a continuum-based finite element model, *Engineering Structures* 31 (10) (2009) 2380–2391.
- [39] D. Z. Yankelevsky, M. Jabareen, A. D. Abutbul, One-dimensional analysis of tension stiffening in reinforced concrete with discrete cracks, *Engineering Structures* 30 (1) (2008) 206–217.
- [40] P. H. Bischoff, Effects of shrinkage on tension stiffening and cracking in reinforced concrete, *Canadian Journal of Civil Engineering* 28 (3) (2001) 363–374.
- [41] G. Kaklauskas, V. Gribniak, D. Bacinskas, P. Vainiunas, Shrinkage influence on tension stiffening in concrete members, *Engineering Structures* 31 (6) (2009) 1305–1312.
- [42] R. I. Gilbert, G. Ranzi, *Time-Dependent Behaviour of Concrete Structures*, London: Spon Press, 2010.
- [43] Z. P. Bažant, S. Baweja, Justification and refinements of model b3 for concrete creep and shrinkage 1. statistics and sensitivity, *Materials and Structures* 28 (7) (1995) 415–430.
- [44] N. Gardner, M. Lockman, Design provisions for drying shrinkage and creep of normal-strength concrete, *ACI Materials Journal* 98 (2) (2001) 159–167.
- [45] N. Gardner, Comparison of prediction provisions for drying shrinkage and creep of normal-strength concretes, *Canadian Journal of Civil Engineering* 31 (5) (2004) 767–775.
- [46] C. euro-international du béton, CEB-FIP model code 1990: design code, no. 213-214, Telford, 1993.

- [47] T. Xiang, C. Yang, G. Zhao, Stochastic creep and shrinkage effect of steel-concrete composite beam, *Advances in Structural Engineering* 18 (8) (2015) 1129–1140.
- [48] T. Xu, T. Xiang, R. Zhao, G. Yang, C. Yang, Stochastic analysis on flexural behavior of reinforced concrete beams based on piecewise response surface scheme, *Engineering Failure Analysis* 59 (2016) 211–222.
- [49] H. Keitel, A. Dimmig-Osburg, Uncertainty and sensitivity analysis of creep models for uncorrelated and correlated input parameters, *Engineering Structures* 32 (11) (2010) 3758–3767.
- [50] JCSS Probabilistic Model Code, Joint committee on structural safety, URL: [www.jcss.ethz.ch](http://www.jcss.ethz.ch).
- [51] Z. P. Bazant, K. L. Liu, Random creep and shrinkage in structures: Sampling, *Journal of Structural Engineering* 111 (5) (1985) 1113–1134.
- [52] B. R. Ellingwood, T. V. Galambos, J. G. MacGregor, C. A. Cornell, Development of a probability based load criterion for American national standard A58, U.S. Dept. of Commerce, National Bureau of Standards, U.S. Govt. Print. Off, Washington, D.C., 1980.
- [53] D. V. Val, L. Chernin, Serviceability reliability of reinforced concrete beams with corroded reinforcement, *Journal of Structural Engineering* 135 (8) (2009) 896–905.
- [54] B. R. Ellingwood, C. G. Culver, Analysis of live loads in office buildings, *American Society of Civil Engineers* 103 (8) (1977) 1551–1560.

- [55] B.-S. Choi, A. Scanlon, P. A. Johnson, Monte carlo simulation of immediate and time-dependent deflections of reinforced concrete beams and slabs, *ACI Structural Journal* 101 (5) (2004) 633–641.
- [56] C. M. Tan, Nonlinear vibrations of cracked reinforced concrete beams, Ph.D. thesis, University of Nottingham (2003).
- [57] S. Law, X. Zhu, Nonlinear characteristics of damaged concrete structures under vehicular load, *Journal of Structural Engineering* 131 (8) (2005) 1277–1285.
- [58] S. Law, X. Zhu, Dynamic behavior of damaged concrete bridge structures under moving vehicular loads, *Engineering Structures* 26 (9) (2004) 1279–1293.
- [59] H. Baji, H. R. Ronagh, Reliability-based study on ductility measures of reinforced concrete beams in aci 318, *ACI Structural Journal* 113 (2) (2016) 373–382.
- [60] R. I. Gilbert, Tension stiffening in lightly reinforced concrete slabs, *Journal of Structural Engineering* 133 (6) (2007) 899–903.
- [61] V. Gribniak, Shrinkage influence on tension-stiffening of concrete structures, Ph.D. thesis, Vilniaus Gedimino technikos universitetas (2009).
- [62] AASHTO, AASHTO LRFD bridge design specifications, Washington DC: American Association of State Highway Transportation Officials, 2002.
- [63] M. G. Stewart, Serviceability reliability analysis of reinforced concrete structures, *Journal of Structural Engineering* 122 (7) (1996) 794–803.

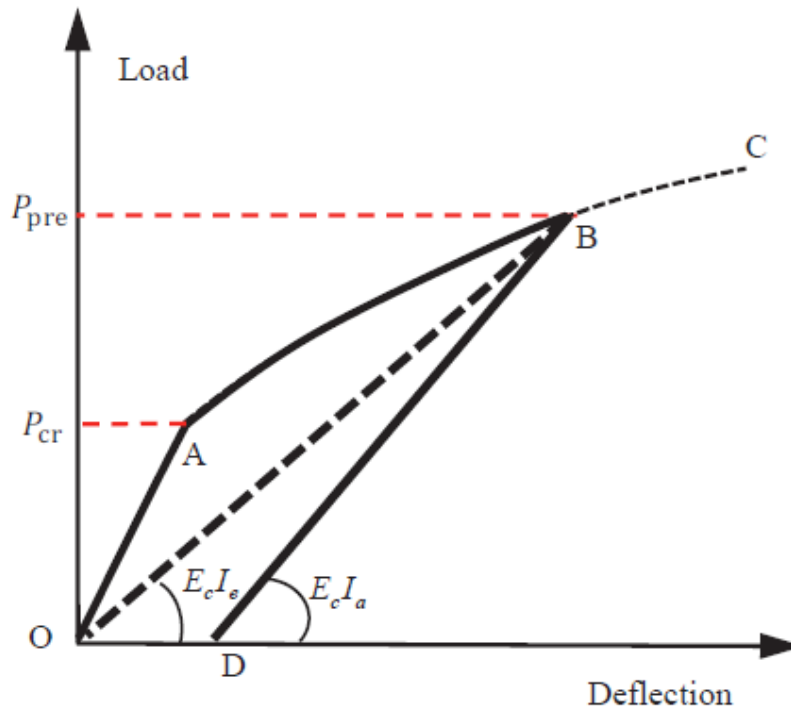


Fig. 1

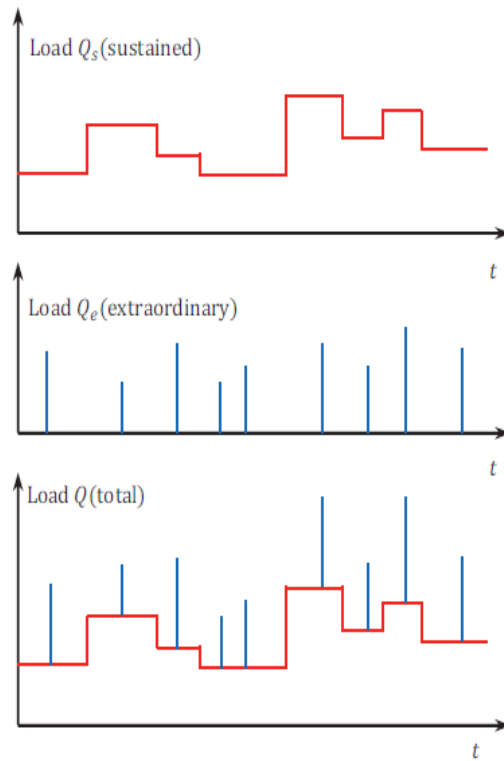


Fig. 2

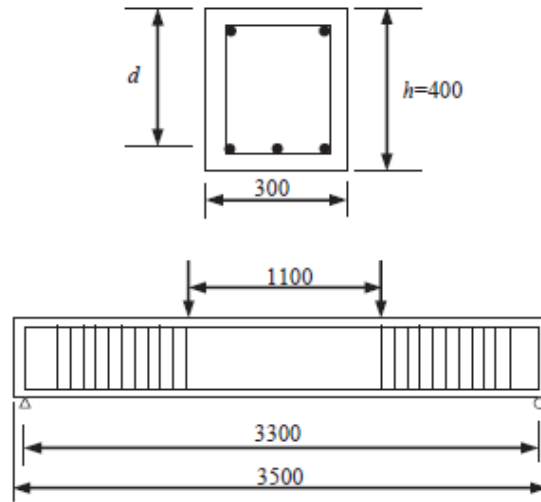


Fig. 3



Fig. 4

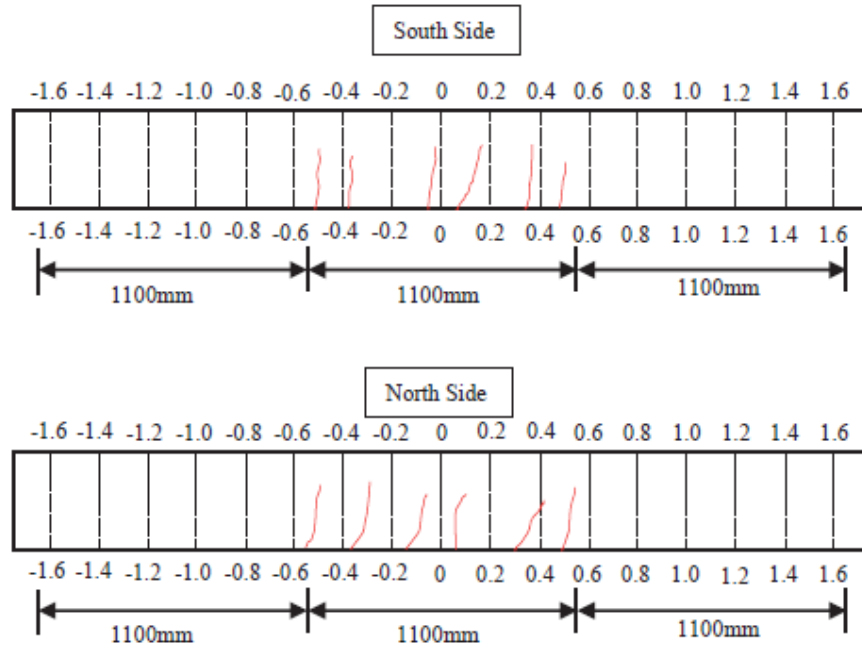


Fig. 5

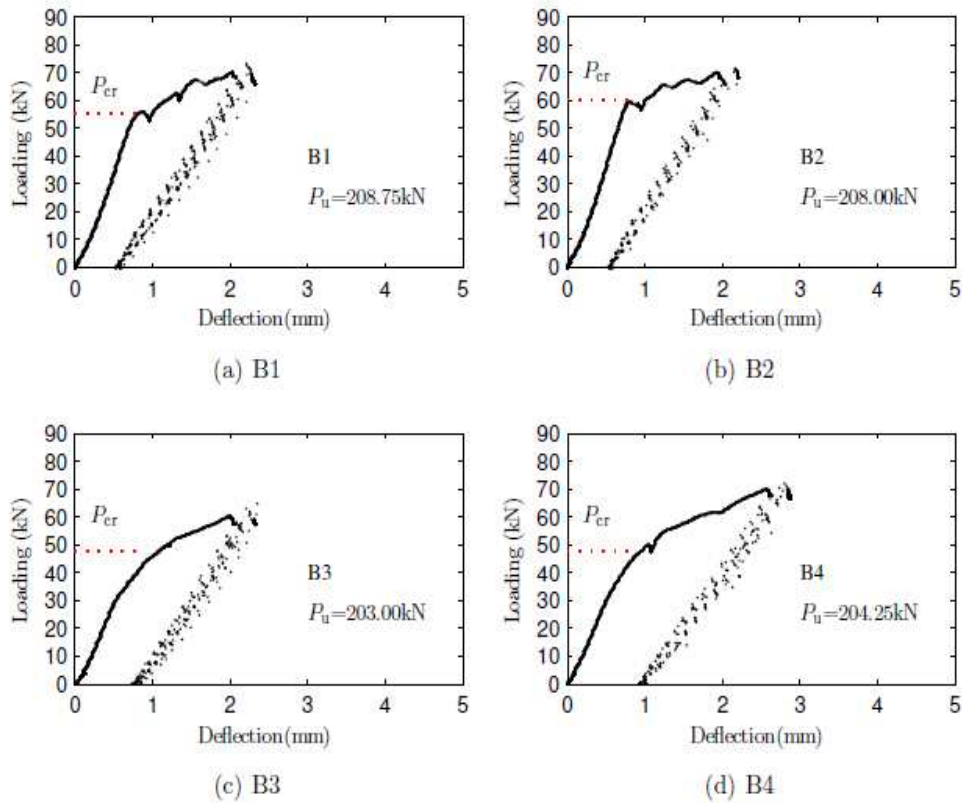


Fig. 6

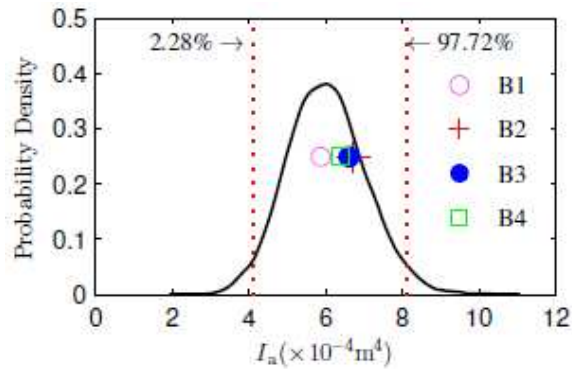
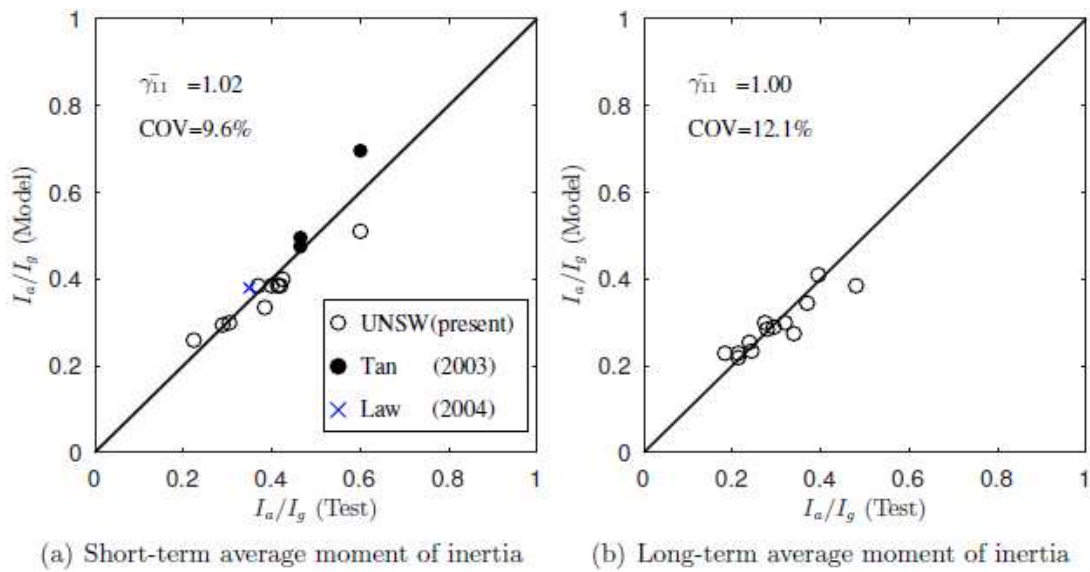


Fig. 7



(a) Short-term average moment of inertia

(b) Long-term average moment of inertia

Fig. 8

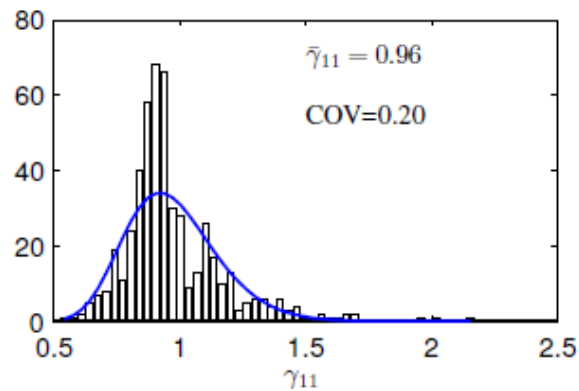


Fig. 9

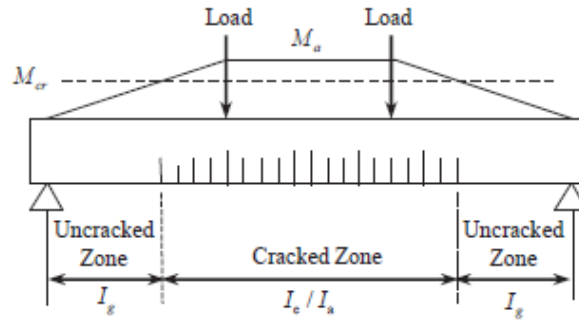


Fig. 10

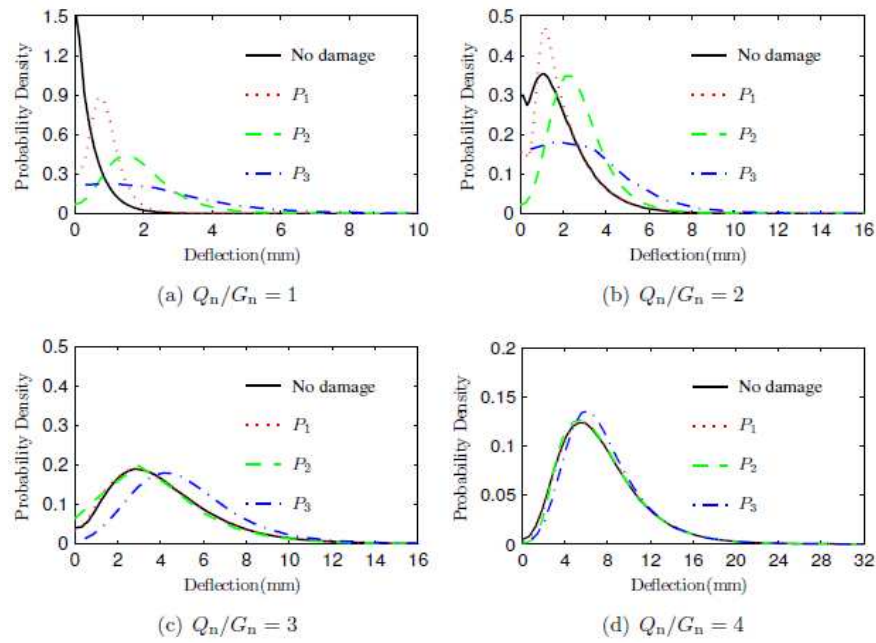


Fig. 11

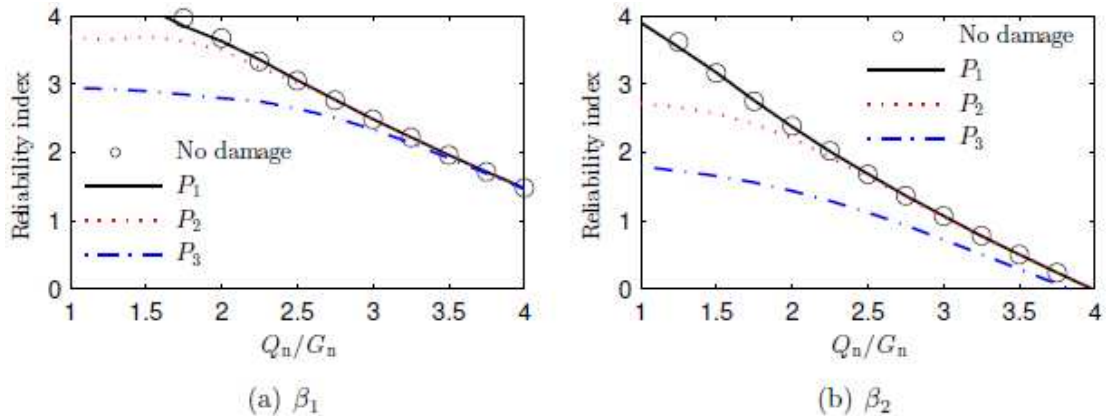


Fig. 12

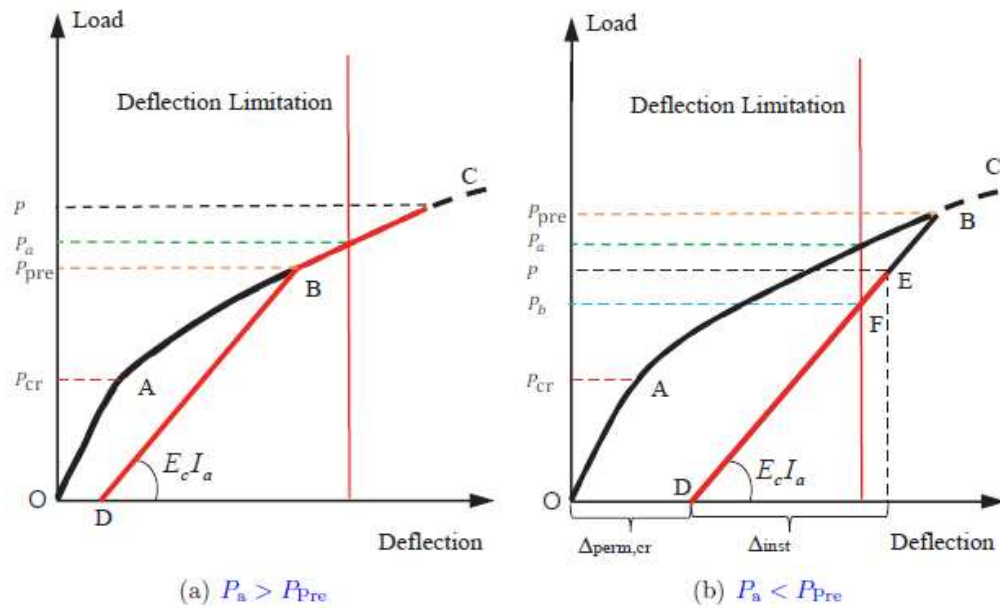


Fig. 13

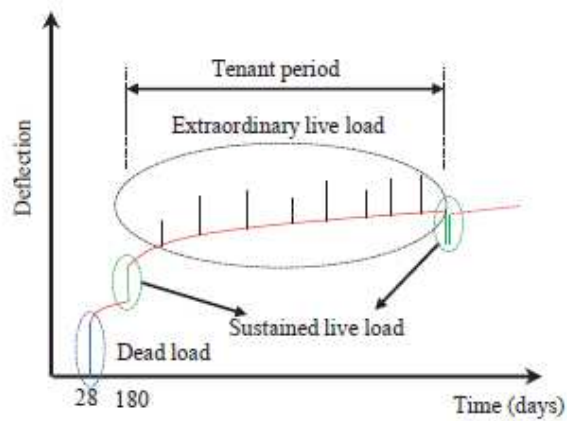


Fig. 14

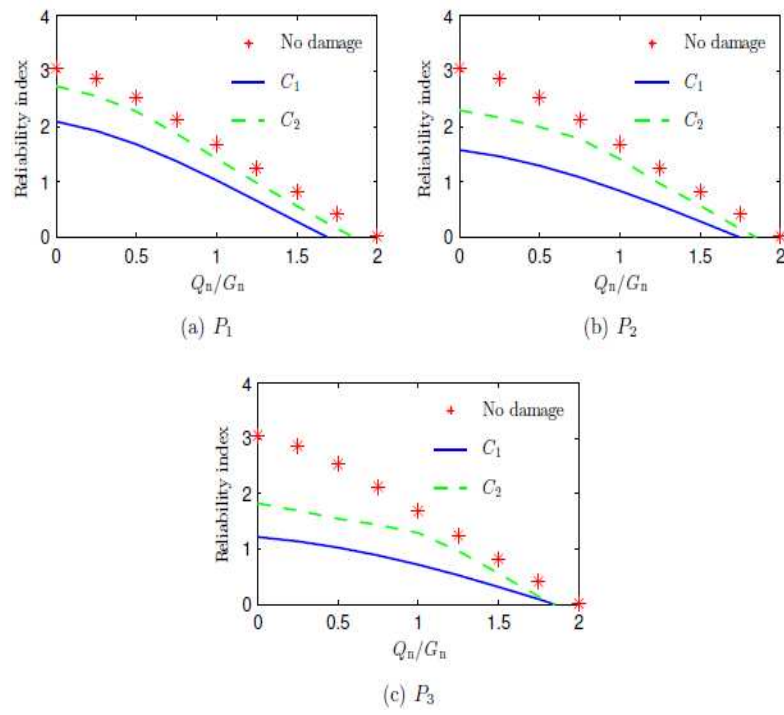


Fig. 15